1. Bartosz PRZYSUCHA[1], 2. Tomasz RYMARCZYK[2,3] 3. Dariusz WÓJCIK[2]

Lublin University of Technology, Nadbystrzycka 38, 20-618 Lublin, Poland (1), Research and Development Center, Netrix S.A., 20-704 Związkowa st. 26, Lublin, Poland (2) University of Economics and Innovation in Lublin, ul. Projektowa 4, 20-209 Lublin, Poland (3)
ORCID. 1. 0000-0002-1117-8088, 2. 0000-0002-3524-9151, 3. 0000-0002-4200-3432

Detection of cardiac arrhythmias in body surface potential mapping (BSMP) measurements

Abstract. The multitude of measurement data obtained from BSPM (Body Surface Potential Mapping) requires automatic detection and classification methods to detect disturbances. The article describes the method of classification of heart rate disorders based on the characteristics of signals from sensors. For the purposes of the research, a coefficient was created that allows the classification of cardiac arrhythmias in the BSPM measurements. In addition, BSPM signals were simulated using a system constructed for testing an innovative measuring vest with 102 measuring electrodes.

Streszczenie. Artykuł opisuje problem klasyfikacji zaburzeń rytmu serca sygnałów otrzymanych z pomiarów BSPM. W pracy skonstruowano współczynnik mierzący dynamikę sygnału I sprawdzono możliwości klasyfikacji sygnału opartej na podstawie wyliczonego współczynnika. Pomiary na baize których dokonano analizy pochodzą z symulacji wykonanych na zaprojektowanym urządzeniu symulacyjnych powstałym w celu testowania innowacyjnej kamizelki pomiarowej BSPM ze 102 elektrodami. (Detekcja zaburzeń rytmu serca w pomiarach potencjału elektrycznego (BSPM)).

Keywords: BSPM measurement, Classification cardiac disease, BSPM signal analysis.
Słowa kluczowe: pomiaryBSPM, analiza sygnału BSPM, klasyfikacja zaburzeń rytmu serca

Introduction

In diagnosing heart rhythm disorders, a frequently used tool is the study of potential maps on the human body. In the ECG, an electric potential at 10 leads/electrode points studies, based on which the specialised staff determines whether abnormalities indicating the disease occurrence could be observed in the signal. In some disorders, the duration of the ECG examination, which usually lasts several minutes, does not allow the observation of the ECG signal distortions based on which the disease could be diagnosed. In such cases, the measuring electrodes are attached for a more extended period, and the patient is equipped with a portable device (holter), that monitors the heart rate over a more extended period. Therefore, there are problems with automatic detection of the measuring signal [2,3] and measurement uncertainty related to the attaching of electrodes or interference factors such as detachment of measuring electrodes or electrostatic friction of clothes. In order to improve the measurement system, a more accurate analysis is applied by wearing a vest equipped with 62 or 102 electrodes. Afterwards, the electrical potential is tested on the entire surface of the patient's torse. Such measurements are referred to in the literature as Body Surface Potential Mapping (BSPM). This method of heart rate monitoring was already carried out in the 1960s [1]. However, due to the level of technology, analysing such a complex signal was limited. Over the last few years, the development of computer technologies and computational capabilities has made that BSPM diagnostics has been the subject of many scientists' research and is presented in many scientific publications [4-13].

The use of the technique based on BSPM with 102 electrodes is a significant advance to standard electrocardiographic examinations based on 3 to 12 channels. Essential for the expansion of myocardial diagnostics are the data from electrodes placed at the heart level. The use of a row of electrodes allows simulating precordial leads (the place where the electrodes from our diagnostic device correspond to the suggested location [14] along with an increase in the surface of these electrodes on the patient's back). In addition, electrodes placed on the surface of the human back allow the data acquisition on the electrical conductivity of the back walls of the heart ventricles. It is essential for diagnosing changes in this area, such as ischemic heart disease or old myocardial infarction. Having multiple electrodes placed at different heights around the heart gives invaluable help in tracking the electrical impulse conductivity within that organ.

This paper deals with the problem of classifying cardiac arrhythmias based on the characteristics of the signal obtained from BSPM measurements. For the classification algorithm, the dynamics coefficient was created.

Material and methods

The simulation system was designed for research on the structure of the BSPM vest. The BSPM measurement vest consists of 102 electrodes made of a conductive textile material embedded in silicone, connected to the measuring system with a ribbon. Obtaining good pressure allowed for better contact with the body and thus for better data readings. The vest was designed by Netrix company and is an innovative solution on a global scale [15,16].

The simulation experiment consisted of collecting appropriate data from devices adapted to generate the simulation: The ProSim 4 ECG simulator was used to generate a stimulation signal of disorders and the normal heart cycle; The phantom converts the 10-lead ECG simulator signal to 102 BSPM distributions; Multiplexer systems connected in series with each other using FFC tape; A controller system, designed to amplify the signal and convert it from analog to digital signal.
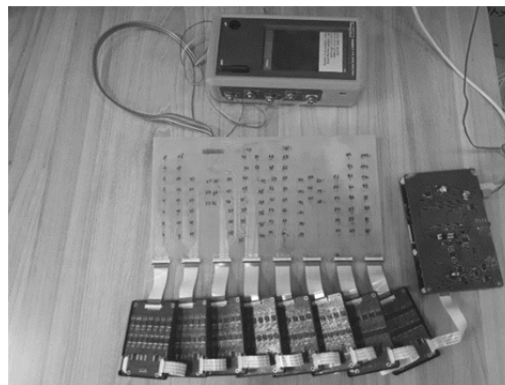
The simulation system is presented in Figure 1.

Fig. 1. BSPM simulation system with connected ECG simulator.

The phantom has 102 leads connected to the ProSim 4 ECG simulator. It is used to generate an ECG signal. The simulator can generate a standard ECG signal, slow heart rate up to 30 BPM, increased heart rate up to 300 BPM and disorders such as atrial fibrillation, premature ventricular contraction, ventricular tachycardia, ventricular fibrillation, transvenous pacer pulse, second-degree AV block, third-degree AV block. The board is designed to convert the ECG signal, using a network of resistors, into a BSPM signal and transfer it to the multiplexer system using FFC tapes. Each board has been designed to be given any address from the range 0-7 to connect up to 8 plates in series, providing up to 128 measurement channels. Each measurement channel has an independent forming and pre-filtration system so that the signal given to the analog keys has a many times greater signal-to-noise ratio than the signal directly measured. Additionally, due to the use of input blocks, the maximum input impedance of the measuring system was ensured. Multiplexers connected in series using FFC tapes collect the signal to the controller system, where the signal is converted into a digital signal, which, after connecting to a computer via USB port, can save it to the hard drive. Fig 1.

The simulation system consists of elements: a simulation plate with 102 measuring points and a plate allowing mechanical integration of measuring electrodes with the simulation Phantom. For this purpose, an integrated circuit of 16 channels was created. Furthermore, as a control element, a snap board system for the discovery development board was constructed, ensuring the integration of measuring electrodes with the control system. In addition to the integration function, the overlay on the discovery board includes a Wilson reference voltage source which, depending on the needs, can be used as a reference voltage signal for signal processing systems, a virtual reference voltage source, a 50Hz middle filter, and control signal amplifier buffers.

The Fluke ProSim 4 ECG signal generator was used as the test signal source at the design stage, which generates signals similar to those measured in real conditions, with a similar level and type of noise as in the case of a real object. Thanks to the available modes, this simulator allows (in addition to checking the correctness of operation) to perform tests for various pulse frequencies and simulate many different cardiovascular diseases. The experiment collected appropriate simulation data, and each measurement of standard myocardial work together with the abnormalities was performed at one-hour intervals.

Signal simulations were performed with the following disturbances: Atrial fibrillation, Bradycardia, Normal signal.

The numbers of measuring signals from each category are in Table 1. fragments of the analysed signals are presented in Figures 2-4.

Table 1. The number of samples of measuring signals with particular disturbances.

Type of disturbance	Sample size
Artial Fibrilation (AFib_Fine)	756885
Bradycardia (Bradycardia_30bpm)	810329
Signal without disturbances (Normal)	716120

In the graphs (Fig. 2-4), the measurement results for individual disturbances are characterised by variable dynamics and amplitude.

Sampled signal values were obtained from the measurement simulations X_k^j from individual channels $\{x_i^j\}$, i=1,...,n − sample item number, j=1,...,102 channel number, k=1,...3 − type of disturbance. The sampling time was 4 ms.
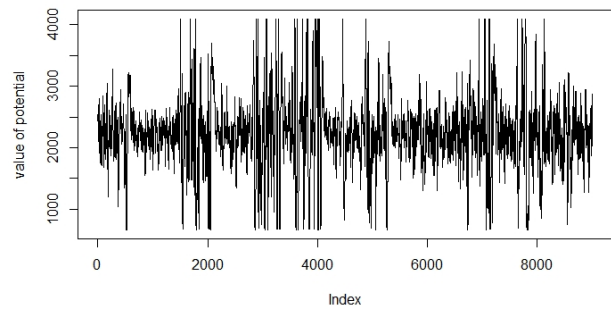

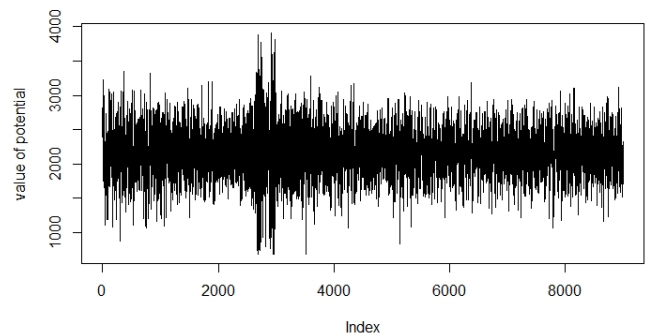Fig 2. Part of the signal with the AFib_Fine disturbance from the first channel.

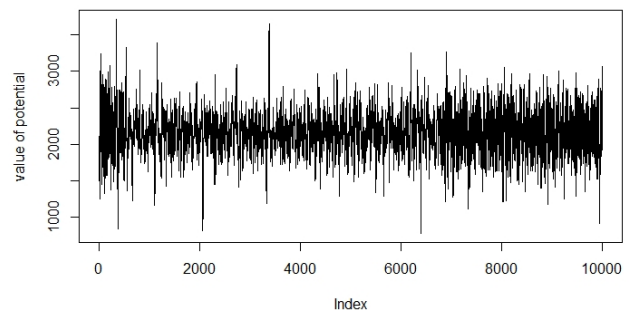Fig. 3. Part of the BSMP signal with Bradycardia_30BPM disturbance from the first channel.

Fig.4. Part of Normal signal without disturbance from the first channel.

For the research, a coefficient was also developed, which allowed examining the signal dynamics - this coefficient is defined by the formula (1)

$$(1) \qquad d_{s,i}^j = \frac{1}{Var(X^j)} \sum_{n=n_i}^{n_i+T-1} |\Delta(x_n^j)|,$$

where $\Delta(x_n^j)$ − is the discrete differential of the signal X^j at the appropriate time slot T.

Whereas $Var(X^j)$ − is the signal variance calculated for the j-th channel from the entire time course.

This coefficient examines the dynamics of the signal. It allows for the calculation of the total speed of change to the changes in amplitude. It is standardised by signal variance to provide the coefficient values with a smaller spread within given disturbances.

In the beginning, the optimal time window for which the above coefficients have the best properties was

determined. Then, time slots of 10 seconds, 20 seconds, 40 seconds, 80 seconds, and 160 seconds were analysed.

Then, the classification possibilities were analysed using the above coefficients for individual channels and the value of the summed dynamics index. Many different algorithms are used to solve optimisation problems [17-26]. The method used for classifying without supervising learning is cluster analysis using the k-means method with euclidean metrics.

The calculations were performed in the R environment using packages dplyr, pracma, tidyverse, cluster, jpeg, corrplot, pkgconfig.

Results

From the determined coefficients calculated for different lengths of the time window, it can be observed that the obtained coefficients stabilise within individual groups of disturbances for the dynamics factor with the lengthening of the time window. Therefore, the optimal time slot with a length of 160 seconds was selected for the analyses in terms of classification analyses. A time window of 160 seconds both reduces the size of the data and provides a sufficient sample size for accurate classification of the measurement signal. For 102 measurement channels, the dynamic coefficient values were calculated with a length of 160 seconds, and 17 values of the dynamic for each signal type were obtained.

The diagram for the summed up the dynamic coefficient for the group of disorders is in Figure 5. The diagram of the dynamic coefficient for 27 channels is in Figure 6.
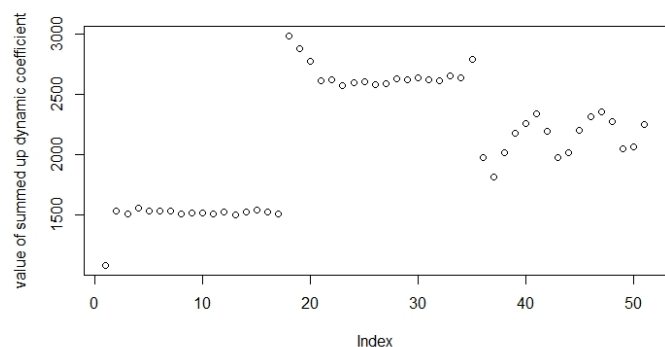

Fig. 5. Diagram of the summed up dynamic coefficient for the group of disorders from left AFib_Fine, Bradycardia, Normal.
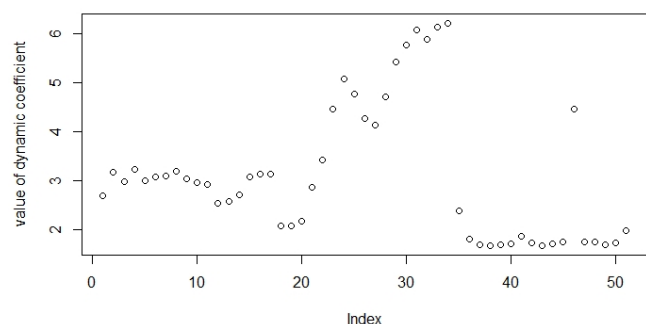

Fig. 6. Diagram of the dynamic coefficient (channel 27) for the group of disorders from left AFib_Fine, Bradycardia, Normal.

The analysis carried out showed the differentiation of the values of the coefficients in particular groups.

In order to check the classification possibilities of the dynamics coefficient, the grouping of the coefficient values was checked using the k-means cluster analysis method.

There are poor classification properties for channels 26-35, 42-43, 67-77. Figure 6 shows the dynamic coefficient for channel 27. For the other channels, the classification coincides with the disorder groups, in particular for Bradycardia. The dynamic coefficient summed up across all channels has the best classification properties in Figure 5.

For the summed dynamic coefficient, a classification possibility study was performed. For this purpose, the classification method without a teacher of k-means cluster analysis with Euclidean metric was used. The number of classes k=3 was assumed. Figure 7 shows the results of clustering the values of the summed dynamic coefficient.
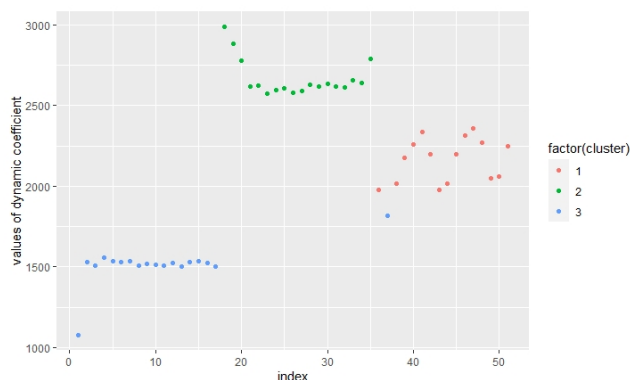

Fig. 7. Classification diagram using the k-means method with a given number of classes k = 3 for the summed up dynamics coefficient for the group of disorder 1. Normal, 2. Bradycardia, 3. AFib_Fine

As shown in Figure 7, except for one value for the normal signal, the algorithm correctly classified all values. The classification results are also presented in the confusion matrix Table 2.

Table 2. Confusion matrix

	Cluster label		
	AFib_Fine	Bradycardia	Normal
AFib_Fine	17		
Bradycardia		17	
Normal	1		16

From the confusion, the matrix can be calculated that the correctness of classification is 98% for the summed index. Thus, it confirms the high classification potential of the dynamics factor in detecting cardiac arrhythmias from BSPM measurements.

Conclusion

The paper analyses the classification possibilities of the dynamics factor in the automatic detection of cardiac arrhythmias. The study was carried out on simulation data obtained from a specially designed simulation system for the innovative BSPM measuring vest. Three types of signals were tested: Normal signal and two disorders, Atrial fibrillation and Bradycardia.

This paper proposes the construction of a dynamic coefficient that measures the amplitude of a signal and its dynamics simultaneously. To improve the classification capabilities of the coefficient, the values are normalised by the variance of the signal.

A cluster analysis method with the Euclidean metric was applied to test the proposed coefficient's classification capabilities. Cluster analysis is a method without a teacher

and allows to check if the values assigned to the groups by the algorithm coincide with the apriori determined values.

The k-means cluster classification method obtained that the summed up dynamics coefficient from all channels had the best classification properties.

The coefficient proposed in this paper gives the possibility for the correct classification of signals coming from BSPM measurements. It can be used as a value to base the learning of artificial intelligence algorithms such as neural networks, classification trees, support vector machines, etc.

Authors: *dr Bartosz Przysucha Lublin University of Technology, Nadbystrzycka 38, 20-618 Lublin, Poland, E mail: b.przysucha@pollub.pl, prof. dr hab. inż. Tomasz Rymarczyk,* Research and Development Center, Netrix S.A., 20-704 Związkowa st. 26, Lublin, Poland, University of Economics and Innovation in Lublin, ul. Projektowa 4, 20-209 Lublin, Poland, E mail: tomasz.rymarczyk@netrix.com.pl; dr Dariusz Wójcik Research and Development Center, Netrix S.A., 20-704 Związkowa st. 26, Lublin, Poland, *E-mail: dariusz.wojcik@netrix.com.pl.*

REFERENCES

[1] Lux R.L., Body Surface Potential Mapping Techniques, In: Macfarlane P.W., van Oosterom A., Pahlm O., Kligfield P., Janse M., Camm J. (eds) Comprehensive Electrocardiology. Springer, London, (2010), https://doi.org/10.1007/978-1-84882-046-3_31

[2] Kłosowski G., Rymarczyk T., Wójcik D., Skowron S., Cieplak T. Adamkiewicz P., The Use of Time-Frequency Moments as Inputs of LSTM Network for ECG Signal Classification, *Electronics* , 9, (2020), 1452, https://doi.org/10.3390/electronics9091452

[3] Przysucha B., Rymarczyk T., Wójcik D., Wos M., Vejar A., Improving the Dependability of the ECG Signal for Classification of Heart Diseases, 2020 50th Annual IEEE-IFIP International Conference on Dependable Systems and Networks-Supplemental Volume (DSN-S), Valencia, Spain, (2020), 63-64, doi: 10.1109/DSN-S50200.2020.00034.

[4] Gronewegen A. S., Lesh M., D, Roithinger F. X., Ellies W.S., Steiner P. R., Saxon L. A., Lee R. J., Schienman M., Body Surface Mapping of Counterlockwise and Clockwise typical Atrial Flutter: A Comparative Analysis Witch Endocardial Activation Sequence Mapping, *Journal of the American College of Cardiology*, 35, (2000), No 5, 1276-1287.

[5] Korneich F., Montauge T. J., Smet P., Rautaharju P. M., Kovadias M., Multigroup diagnostic classification using body surface potential maps, in Proceedings Computers in Cardiology, Jerusalem, Israel, (1989), 181-184. Doi: 10.1109/CIC.1989.130516

[6] Hänninen H., Takala P., Rantonen J., Mäkijärvi M., Virtanen K., Nenonen J., Katila T., Toivonen L., ST-T integral and T-wave amplitude in detection of exercise-induced myocardial ischemia evaluated with body surface potential mapping, *Journal of Electrocardiology*, 36, (2003), No 2, 89-98.

[7] Hoekema R., Gurlek C., Brouwer M. A., Chaikovsky I., Verheugt F. W. A., The use of magnetocardiography and body surface potential mapping in the detection of coronary artery disease in chest pain patients with a normal electrocardiogram, *Computers in Cardiology,* Chicago, IL, USA, (2004), 389-392, doi: 10.1109/CIC.2004.1442954.

[8] Polak-Jonkisz D., Laszki-Szcząchor K., Purzyc L., Zwolińska D., Musiał K., Pilecki W., Rusiecki L., Janocha A., Kałka D., Sobieszczańska M., Usefulness of body surface potential mapping for early identification of the intraventricular conduction disorders in young patients with chronic kidney disease, *Journal of Electrocardiology*, 42, (2009), No 2, 165-171.

[9] Korhonen P., Husa T., Konttila T., Tierala I., Mäkijärvi M., Väänänen H., Toivonen L., Complex T-wave morphology in body surface potential mapping in prediction of arrhythmic events in patients with acute myocardial infarction and cardiac dysfunction, *EP Europace*, 11, (2009), No 4, 514–520, https://doi.org/10.1093/europace/eup051

[10] Zarychta P., Smith F.E., King S.T., Haigh A.J., Klinge A., Zheng D., Stevens S., Allen J., Okelarin A., Langley P., Murray A., Body Surface Potential Mapping for Detection of Myocardial Infarct Sites, *Computers in Cardiology*, 34, (2007), 181−184.

[11] Dalay M. J, Finaly D. D., Scott P.J., Nugent C. D., Adgey A. A. J., Haribson M. T., Pre-hospital body surface potential mapping improves early diagnosis of acute coronary artery occlusion in patients with ventricular fibrillation and cardiac arrest, *Resuscitation*, 84, (2013), No 1, 37-41, https://doi.org/10.1016/j.resuscitation.2012.09.008.

[12] Simelius K., Stenroos M., Reinhardt L., Nenonen J., Tierala I., Mäkijärvi M., Toivonen L., Katila T., Spatiotemporal characterisation of paced cardiac activation with body surface potential mapping and self-organising maps, *Physiological Measurement*, 24, (2003), No 3, 805-8016, https://doi.org/10.1088/0967-3334/24/3/315.

[13] Rodrigo M., Climent A.M., Liberos A., Fernández-Aviles F., Atienza F., Guillem M.S., Berenfeld O., Minimal configuration of body surface potential mapping for discrimination of left versus right dominant frequencies during atrial fibrillation, *Pacing Clin Electrophysiol*. 40, (2017), No 8, 940-946. doi: 10.1111/pace.13133.

[14] Wójcik D., Kozłowski E., Woś M., Rymarczyk T., Wośko E., Machine Lerning Pathology Detection with a Body Surface Potential Mapping, UbiComp-ISWC '20 : Adjunct Proceedings of the 2020 ACM International Joint Conference on Pervasive and Ubiquitous Computing and Proceedings of the 2020 ACM International Symposium on Wearable Computers / gen. chairs: Monica Tentori, Nadir Weibel, Kristof Van Laerhoven.- New York : Association for Computing Machinery (ACM), (2020), 151-155, https://doi.org/10.1145/3410530.3414404

[15] Robinson M. R., Curzen N., Electrocardiographic body surface mapping: Potential tool for the detection of transient myocardial ischemia in the 21st century, Annals of Noninvasive Electrocardiology, 2009, 14, (2009), 201-210 DOI: 10.1111/j.1542-474X.2009.00284.x

[16] Rymarczyk T., Woś M., Bartosik M., Vejar A., Kozłowski E., Maj M., Electrical activity with ECG analysis for Body Surface Potential Mapping, *Przegląd Elektrotechniczny,* 96, No 10, (2020), 144-147, doi:10.15199/48.2020.10.26

[17] Rymarczyk T.: Characterization of the shape of unknown objects by inverse numerical methods, Przegląd Elektrotechniczny, 88(7B), 138-140,2012.

[18] Rymarczyk, T Using electrical impedance tomography to monitoring flood banks 16th International Symposium on Applied Electromagnetics and Mechanics (ISEM),International journal of applied electromagnetics and mechanics 45, 489-494,2014.

[19] Filipowicz, SF and Rymarczyk, The Shape Reconstruction of Unknown Objects for Inverse Problems Przegląd Elektrotechniczny, 88 (3A), 55-57,2012.

[20] Koulountzios P., Rymarczyk T., Soleimani M., A quantitative ultrasonic travel-time tomography system for investigation of liquid compounds elaborations in industrial processes, Sensors, 19(23), 5117, 2019.

[21] Kłosowski G., Rymarczyk T., Kania K., Świć A., Cieplak T., Maintenance of industrial reactors based on deep learning driven ultrasound tomography, Eksploatacja i Niezawodnosc – Maintenance and Reliability; 22(1), 138–147, 2020.

[22] Kłosowski G., Rymarczyk T., Cieplak T., Niderla K., Skowron Ł., Quality Assessment of the Neural Algorithms on the Example of EIT-UST Hybrid Tomography, Sensors, 20(11), 3324, 2020.

[23] Łukiański, M., & Wajman, R. (2020). The diagnostic of two-phase separation process using digital image segmentation algorithms. Informatyka, Automatyka, Pomiary W Gospodarce I Ochronie Środowiska, 10(3), 5-8.

[24] Duraj, A.; Korzeniewska, E.; Krawczyk, A. Classification algorithms to identify changes in resistance. Przegląd Elektrotechniczny 2015, 1, 82–84.

[25] Krawczyk, A.; Korzeniewska, E. Magnetophosphenes–history and contemporary implications. Przegląd Elektrotechniczny 2018, 1, 63–66.

[26] Mosorov, V ; Rybak, G ; Sankowski, D, Plug Regime Flow Velocity Measurement Problem Based on Correlability Notion and Twin Plane Electrical Capacitance Tomography: Use Case, Sensors Volume: 21 Issue: 6 Article Number: 2189 DOI: 10.3390/s21062189, 2021.